Evaluation of ECAL potential in Differentiating the Signal from the Neutrino-induced Background in SHiP experiment

Ryotaro Shinoda*
The University of Tokyo, Institute of Cosmic Ray Research, Japan

Supervised by Dr. Iaroslava Bezshyiko
(Dated: September 23, 2024)

The Search for Hidden Particle (SHiP) experiment is a fixed target experiment that will be located at Super Proton Synchrotron (SPS) at European Organization for Nuclear Research (CERN). The SHiP experiment will probe new physics in intensity frontier by searching for feebly interacting particles. This study aimed to compare the calorimeter response between the signal and the neutrino-induced background, and apply this information for the signal selection.

I. THEORETICAL BACKGROUND

The standard model of elementary particles (SM) is the theory which describes electromagnetic, weak and strong interactions. It has remained consistent with many experimental facts up to date. Also, it allows for massive gauge bosons through spontaneous symmetry breaking while conserving gauge invariance. However, the SM can not explain some observed phenomena such as dark matter, neutrino oscillation, baryon asymmetry of the universe.

A. Hidden sector classification

There are several ways to approach these problems. One way is to add some renormalizable interaction terms (portal) to the SM lagrangian. The following discusses the portals which the SHiP experiment is capable of exploring. In addition to these examples, the SHiP experiment is also sensitive to axion-like particles and light supersymmetric particles.

1. Vector portal

It is possible to add $U(1)$ gauge structure (vector portal) to the SM. Under the new gauge symmetry, the new charged gauge boson (dark photon) is introduced. The interaction term of the vector portal to the SM can be expressed by the kinematic mixing: $\epsilon F_{\mu\nu}F'_{\mu\nu}$ Where ϵ is the portal coupling. Dark photon can be a dark matter mediator and it also possibly explains muon $g-2$ anomaly. [1]

2. Scalar portal

The scalar portal S can be introduced as its interaction term to the SM: $(\alpha_1 S+\alpha S^2)(H^\dagger H)$. Where α and α_1 are the portal couplings to the SM higgs doublet H. Dark scalar and dark higgs are candidate examples of the scalar portal.[1]

3. Neutrino portal

The neutrino portal N_I ($I = 1, 2, ...\mathcal{N}$) can be introduced as its interaction term to the SM as: $F_{\alpha I}\bar{L}_\alpha N_I \tilde{\Phi}$. Where $F_{\alpha I}$ is a Yukawa coupling, L_α is the left-chiral lepton doublet, α denotes the flavor index and $\tilde{\Phi}$ is the VEV of higgs doublet.[1] In the $\mathcal{N} = 3$ case, three right-chiral neutrinos are added to the SM particles. This model is called the neutrino minimal standard model ($\nu_{\rm MSN}$). It can explain simultaneously dark matter and baryon asymmetry of the universe, and it is consistent with neutrino oscillation experiments.[2] In the $\nu_{\rm MSN}$, a light N_1 with a mass of $\mathcal{O}(10)$ keV is decoupled with the other N_i. And two Heavy Neutral Leptons (HNLs) $N_{2,3}$ with a mass of $\mathcal{O}(1)$ GeV weakly coupled to the SM particles. $N_{2,3}$ are predicted to have the decay channel in which they decay into the SM particles in the energy scale which is going to be probed by SHiP.

Table I. Possible portal interaction terms.

Portal	Interaction term
Vector	$\epsilon F_{\mu\nu}F'_{\mu\nu}$
Scalar	$(\alpha_1 S + \alpha S^2)(H^\dagger H)$
Neutrino	$F_{\alpha I}\bar{L}_\alpha N_I \tilde{\Phi}$

II. THE SHIP EXPERIMENT

The SHiP is a proposed heavy fixed target experiment which will be located at ECN3 cavern at SPS accelarator.[3] The experiment is designed to search for the feebly interacting long-lived particles with masses below $\mathcal{O}(10)$ GeV, such as HNLs, dark photons, dark scalars, axion-like particles and light supersymmetric particles in the intensity frontier. The experiment will also carry the dedicated detector for τ neutrinos physics.

* shinoda@km.icrr.u-tokyo.ac.jp

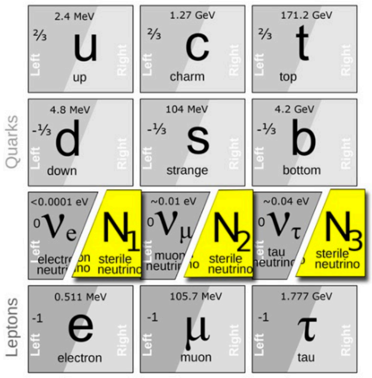

Figure 1. The ν_{MSN} particles[1]. Three right-chiral neutrinos are added to the SM particles as the neutrino portal.

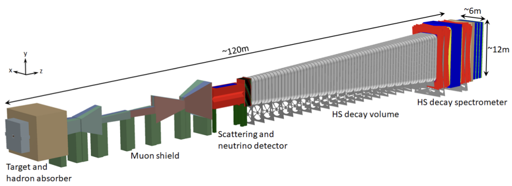

Figure 2. The geometry of the SHiP detector in the simulation [4]

400 GeV proton beam from SPS accelarator will be directed on the Titanium-Zirconium doped Molybdenum target. The target is followed by the hadron absorber and the muon shield which deflects muons out of the detector acceptance to provide background free environment. The SHiP detector is going to consists of two main parts:

- Hidden Sector Decay Spectrometer (HSDS)
- Scattering and Neutrino Detector (SND)

The SND is desinged to provide the neutrino physics studies. The HSDS is designed to measure the decay products of the hidden sector particles which reconstructed vertices are in the 50 m long decay volume at the upstream. In the hidden sector detector, the electromagnetic calorimeter (ECAL) is going to be located the downstream of the decay volume to provide particle identification and timing information, and to measure energies of electrons and photons. The main background sources in the SHiP experiment are:

- Neutrino deep-inelastic scattering
- Muon inelastic scattering (including cosmic ray muon)

These background can be observed in the ECAL and can mimic the signal. In this study, the possibility to utilize these information from the ECAL to separate a signal candidate from the background was evaluated.

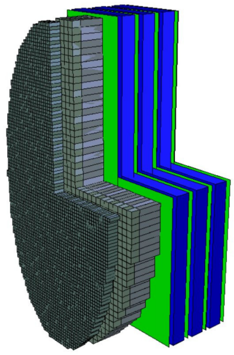

Figure 3. The overview of the ECAL [4]

III. SIMULATION METHODS

FairSHiP is a dedicated framework for the simulation and reconstruction of the SHiP experiment[5]. It is based on FairROOT[6] and incorporates several monte carlo generators to simulate precisely different interactions:

- GENIE (For reading and processing neutrino interactions)
- PYTHIA8
- PYTHIA6

Signals and backgrounds are separately generated in the simulation. The ECAL cluster, digitised information which has spatial and deposited energy informationis is generated when each particle hits the ECAL. Each event consists of ECAL clusters that are coming from the same initial interaction.

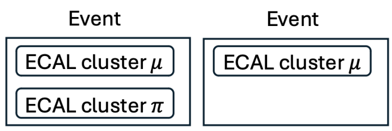

Figure 4. Concept of events and ECAL clusters

IV. RESULTS

In this study, the difference of the cluster distribution in the ECAL between HNL-induced clusters and neutrino-induced clusters was evaluated. We used the signal mode of HNLs ($N_{2,3} \to \mu^{\pm}\pi^{\mp}$) and neutrino-induced backgrounds. Neutrinos were chosen becasuse they may enter the decay volume without being detected by the veto system. Both, signal and background samples, were simulated for two cases: with decay volume kept under pressure and filled with helium. The reason for this is explained by the current studies on relaxing the vacuum level. We have used three parameters to characterise the ECAL respond for each event:

- Average energy deposited by cluster per event
- Highest energy deposited by cluster per event
- Number of clusters per event

Table II. The number of events reconstructed as the signal at the ECAL. For each case except the neutrino-induced background under vacuum, 10.0k events are forced to interact at the ECAL. (20.0k events for the neutrino-induced background under vacuum.) Neutrino-induced events are misidentified as signals by the following numbers.

-	Vacuum	Helium
HNLs	3.8k	3.9k
Neutrino	1.2k	0.6k

A. Decay Volume kept under vacuum

Figure 5 shows the average energy deposited by cluster per event, while Figure 6 shows the highest energy deposited by cluster per event. In both figures, the energy deposition spectrum for HNL-induced events is shifted towards higher energy regions compared to neutrino-induced events. Table III shows the fraction of signals selected when energy cuts are set at 0.3, 0.5, and 1.0 GeV for the average energy. Similarly, Table IV shows the fraction of signals selected with the same energy cuts applied to the highest energy. Figure 9 shows the number of clusters per event, and Table V shows the probability of having N or more clusters within a single event. Notably, for events with two clusters, the probability of detecting HNL events is four times greater than that for neutrino events. This is primarily due to the generation of signals with two decay particles ($N_{2,3} \rightarrow \mu^{\pm}\pi^{\mp}$). Particle types of the ECAL cluster is shown in table VI. HNL-induced clusters mainly consist of muon and pion, due to the signal we generated. Regarding neutrino-induced clusters, they also contain muon and pion, but the ratio of particles to anti particles is not nearly 1. And also they contain more photons than HNL-induced ones.

B. Decay volume filled with helium

A similar trend holds in the case of helium as in the case of vacuum, regarding: average 10 (highest 11) energy deposited by cluster per Event, fraction of signals selected when energy cuts are set III (IV), number of clusters per event 14 and probability of having N or more clusters within a single event IX, Regarding particle types of the ECAL cluster X, muon is far dominant for the HNL-induced clusters.

V. CONCLUSION

In this study, we have evaluated the number of clusters and energy for the HNLs/neutrino-induced events in ECAL. Comparing the averaged/highest energy deposition in the ECAL, the HNL signal shifted into the higher energy region in comparison to the neutrino-induced events in both vacuum and helium cases. In the case of two clusters events, probability of it being a HNL-induced event is four times greater being a neutrino-induced event, and 80% of neutrino-induced events have only one cluster, while 40% of HNL-induced events have only one cluster in both vacuum and helium cases. As a future prospect, the information of cluster position and energy deposition can be used for training a simple network to background separation.

REFERENCES

[1] The SHiP Collaboration, *A facility to Search for Hidden Particles at the CERN SPS: the SHiP physics case* (The SHiP Collaboration, April 2015). URL: `http://arxiv.org/abs/1504.04855`.

[2] Takehiko Asaka, Mikhail Shaposhnikov, *The νMSM, Dark Matter and Baryon Asymmetry of the Universe* (Phys.Lett.B620:17-26,2005). URL: `https://arxiv.org/abs/hep-ph/0505013`.

[3] BDF Working Group, SHiP Collaboration, *BDF/SHiP at the ECN3 high-intensity beam facility* (BDF Working Group, SHiP Collaboration, November 2022). URL: `https://cds.cern.ch/record/2839677?ln=en`.

[4] The SHiP Collaboration, *The SHiP experiment at the proposed CERN SPS Beam Dump Facility* (The SHiP Collaboration, May 2022). URL: `https://arxiv.org/pdf/2112.01487`.

[5] *FairSHiP* URL: `https://ship.web.cern.ch/FairShip`.

[6] *FairRoot* URL: `https://fairroot.gsi.de`.

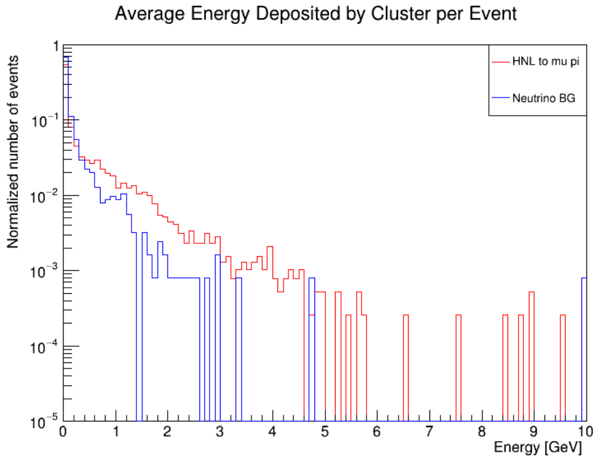

Figure 5. Average energy deposited by cluster per Event in the vacuum case. The histogram is normalized by whole number of events.

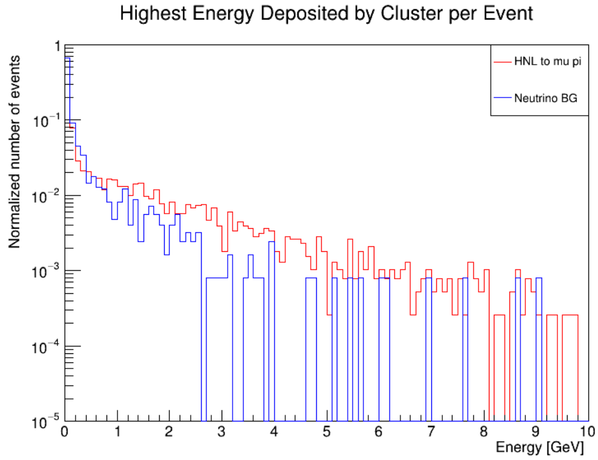

Figure 6. Highest energy deposited by cluster per Event in the vacuum case. The histogram is normalized by whole number of events.

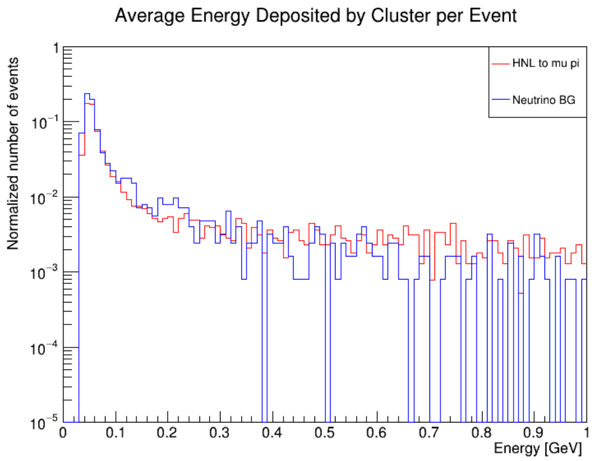

Figure 7. Average energy deposited by cluster per Event below 1 GeV in the vacuum case. The histogram is normalized by whole number of events.

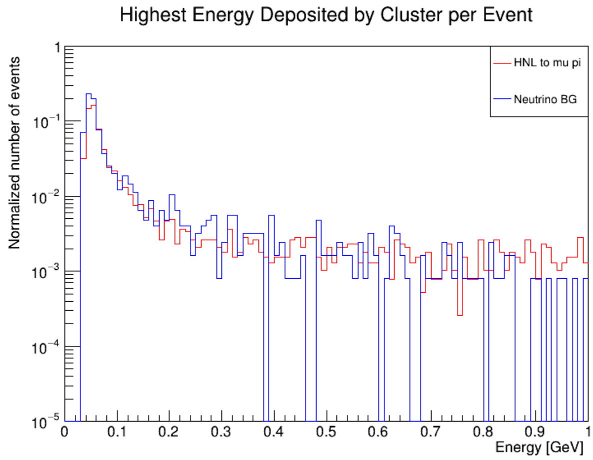

Figure 8. Highest energy deposited by cluster per Event below 1 GeV in the vacuum case. The histogram is normalized by whole number of events.

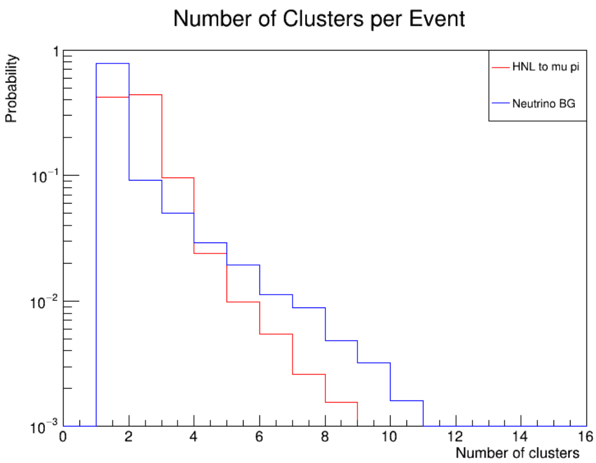

Figure 9. The number of clusters per Event in the vacuum case. The histogram is normalized by whole number of events.

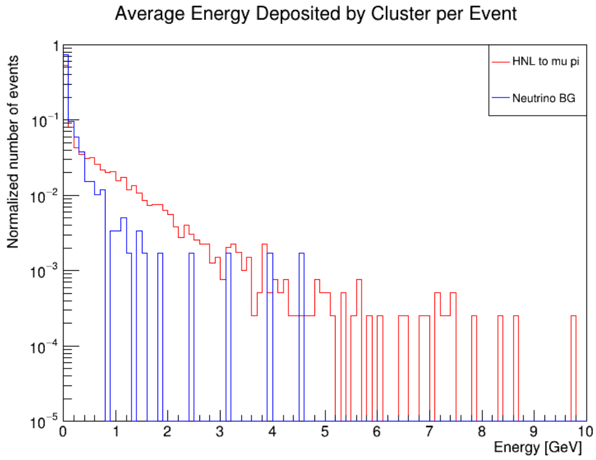

Figure 10. Average energy deposited by cluster per Event in the helium case. The histogram is normalized by whole number of events.

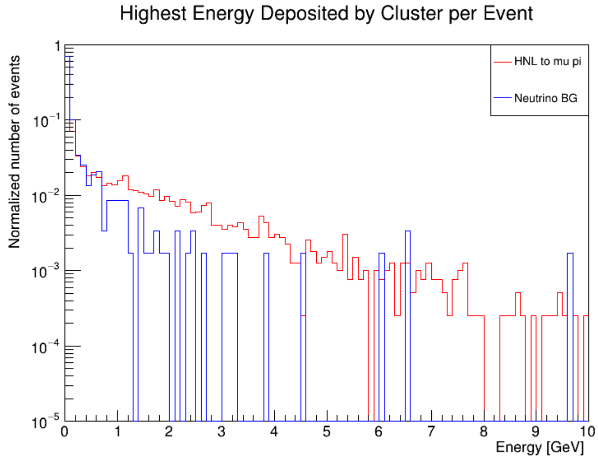

Figure 11. Highest energy deposited by cluster per Event in the helium case. The histogram is normalized by whole number of events.

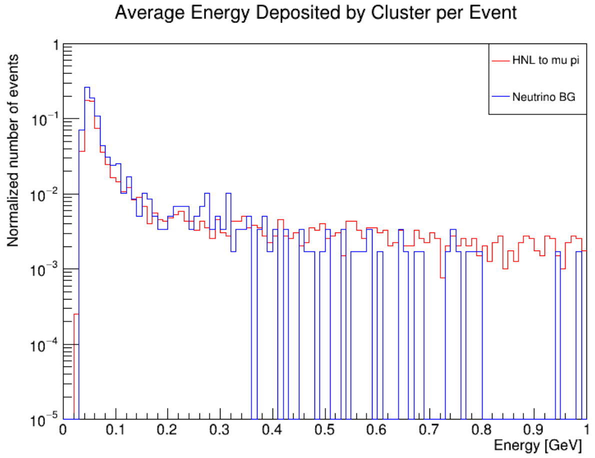

Figure 12. Average energy deposited by cluster per Event below 1 GeV in the helium case. The histogram is normalized by whole number of events.

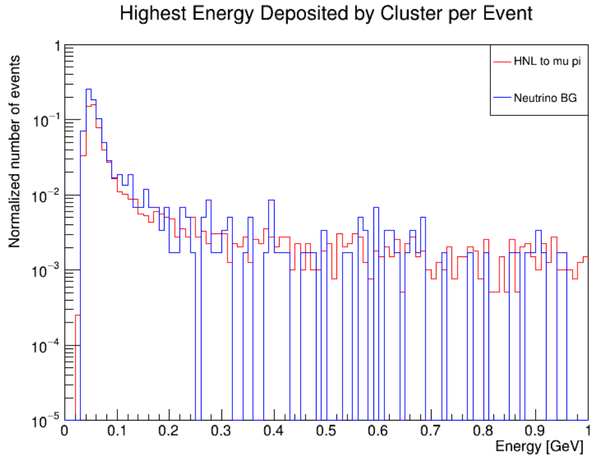

Figure 13. Highest energy deposited by cluster per Event below 1 GeV in the helium case. The histogram is normalized by whole number of events.

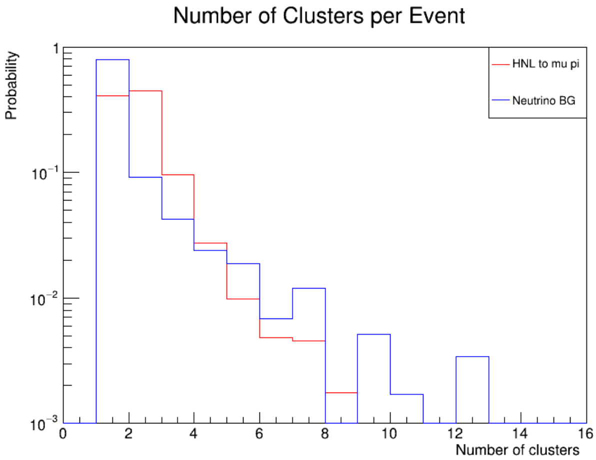

Figure 14. The number of clusters per Event in the helium case. The histogram is normalized by whole number of events.

Table III. The ratio of events with the averaged energy of cluster per event is below $0.3, 0.5, 1.0$ GeV in the vacuum case.

-	< 0.3 GeV	< 0.5 GeV	< 1.0 GeV
HNLs	67%	73%	86%
Neutrino	84%	89%	95%

Table IV. The ratio of events with the highest energy of cluster per event is below $0.3, 0.5, 1.0$ GeV in the vacuum case.

-	< 0.3 GeV	< 0.5 GeV	< 1.0 GeV
HNLs	62%	66%	75%
Neutrino	80%	88%	90%

Table V. The probability of having N or more clusters within a single event in the vacuum case.

-	$N \geq 1$	≥ 2	≥ 3	≥ 4	≥ 5
HNLs	100%	58%	14%	4%	2%
Neutrino	100%	22%	13%	8%	5%

Table VI. Particle types of the ECAL cluster in the vacuum case.

-	μ^-	μ^+	π^-	π^+	e^-	e^+	K^-	K^+	γ	proton	neutron
HNLs	23.7%	23.8%	21.9%	21.3%	0.7%	0.6%	0.2%	0.1%	2.7%	1.6%	1.7%
Neutrino	38.4%	3.1%	8.0%	11.3%	4.4%	4.1%	0.3%	0.4%	15.4%	7.0%	3.7%

Table VII. The ratio of events with the averaged energy of cluster per event is below $0.3, 0.5, 1.0$ GeV in the helium case.

-	< 0.3 GeV	< 0.5 GeV	< 1.0 GeV
HNLs	66%	72%	84%
Neutrino	89%	94%	98%

Table VIII. The ratio of events with the highest energy of cluster per event is below $0.3, 0.5, 1.0$ GeV in the helium case.

-	< 0.3 GeV	< 0.5 GeV	< 1.0 GeV
HNLs	61%	65%	73%
Neutrino	84%	88%	94%

Table IX. The probability of having N or more clusters within a single event in the helium case.

-	$N \geq 1$	≥ 2	≥ 3	≥ 4	≥ 5
HNLs	100%	59%	14%	5%	2%
Neutrino	100%	20%	11%	7%	5%

Table X. Particle types of the ECAL cluster in the helium case.

-	μ^-	μ^+	π^-	π^+	e^-	e^+	K^-	K^+	γ	proton	neutron
HNLs	49.9%	49.9%	< 0.1%	< 0.1%	< 0.1%	< 0.1%	< 0.1%	< 0.1%	< 0.1%	< 0.1%	< 0.1%
Neutrino	44.1%	2.5%	5.9%	10.0%	4.1%	5.0%	0.3%	1.0%	15.0%	5.7%	3.4%